

## BASIC SCIENCE ARTICLE



# Infection of the murine placenta by *Listeria monocytogenes* induces sex-specific responses in the fetal brain

 Kun Ho Lee<sup>1</sup>, Matti Kiupel<sup>2</sup>, Thomas Woods<sup>2</sup>, Prachee Pingle<sup>3</sup> and Jonathan Hardy<sup>3,4</sup>✉

© The Author(s), under exclusive licence to the International Pediatric Research Foundation, Inc 2022

**BACKGROUND:** Epidemiological data indicate that prenatal infection is associated with an increased risk of several neurodevelopmental disorders in the progeny. These disorders display sex differences in presentation. The role of the placenta in the sex-specificity of infection-induced neurodevelopmental abnormalities is not well-defined. We used an imaging-based animal model of the bacterial pathogen *Listeria monocytogenes* to identify sex-specific effects of placental infection on neurodevelopment of the fetus.

**METHODS:** Pregnant CD1 mice were infected with a bioluminescent strain of *Listeria* on embryonic day 14.5 (E14.5). Excised fetuses were imaged on E18.5 to identify the infected placentas. The associated fetal brains were analyzed for gene expression and altered brain structure due to infection. The behavior of adult offspring affected by prenatal *Listeria* infection was analyzed.

**RESULTS:** Placental infection induced sex-specific alteration of gene expression patterns in the fetal brain and resulted in abnormal cortical development correlated with placental infection levels. Furthermore, male offspring exhibited abnormal social interaction, whereas females exhibited elevated anxiety.

**CONCLUSION:** Placental infection by *Listeria* induced sex-specific abnormalities in neurodevelopment of the fetus. Prenatal infection also affected the behavior of the offspring in a sex-specific manner.

*Pediatric Research* (2023) 93:1566–1573; <https://doi.org/10.1038/s41390-022-02307-1>

**IMPACT:**

- Placental infection with *Listeria monocytogenes* induces sexually dichotomous gene expression patterns in the fetal brains of mice.
- Abnormal cortical lamination is correlated with placental infection levels.
- Placental infection results in autism-related behavior in male offspring and heightened anxiety levels in female offspring.

**INTRODUCTION**

Epidemiological data indicate that prenatal infection with bacterial, viral, or parasitic pathogens during pregnancy is associated with an increased risk of neuropsychiatric disorders in the progeny, including autism spectrum disorder (ASD<sup>1</sup>) and schizophrenia.<sup>2,3</sup> Injection of the bacterial endotoxin lipopolysaccharide (LPS) or polyinosinic-polycytidylic acid [poly(I:C)], which mimics viral infections, activates the immune system of pregnant rodents and results in altered brain gene expression<sup>4</sup> and atypical behavior in offspring.<sup>5</sup> These behavioral abnormalities are notably relevant to ASD core symptoms, such as repetitive behaviors and deficits in social interaction. Furthermore, animal studies show sex-biased behaviors and responses in offspring after exposure to the chemical immunogens LPS and poly(I:C) during pregnancy, which resembles sex differences in neuropsychiatric disorders, including ASD.<sup>6,7</sup> Maternal immune activation (MIA) induced by LPS or poly(I:C) causes changes in fetal brain development. However, actual prenatal pathogens exhibit tissue and cell-specificity as well as

directed immune modulation, such that the different pathogens may induce MIA differently. For example, infection of rats with Group B *Streptococcus* (GBS) elicits distinct MIA patterns including neutrophil infiltrates that differ from chemical MIA stimulants.<sup>8</sup> In addition, prenatal influenza is a risk factor for schizophrenia,<sup>2</sup> whereas no such association was found with prenatal infection with either maternal type 2 herpes simplex virus<sup>9</sup> or cytomegalovirus.<sup>10</sup> Thus, the induction of MIA is complex and cannot be completely replicated by any single approach.

*Listeria monocytogenes* (*Lm*) provides an excellent animal model for prenatal infection.<sup>11,12</sup> This Gram-positive bacterium is a foodborne pathogen and is a significant health concern during pregnancy because pregnant women are up to 10 times more likely to be infected with *Lm*.<sup>13</sup> An important hallmark of prenatal listeriosis is the infection of the placenta, which is the main target of *Lm* infection in the reproductive system.<sup>14–16</sup> Placental infection by *Lm* can lead to many overt fetal and newborn pathologies, including spontaneous abortions, neonatal meningitis, a severe

<sup>1</sup>Department of Computational Medicine and Bioinformatics, University of Michigan, Ann Arbor, MI, USA. <sup>2</sup>Department of Pathology and Diagnostic Investigation, Michigan State University, East Lansing, MI, USA. <sup>3</sup>Institute for Quantitative Health and Science Engineering, Michigan State University, East Lansing, MI, USA. <sup>4</sup>Department of Microbiology and Molecular Genetics, Michigan State University, East Lansing, MI, USA. ✉email: [hardyjon@msu.edu](mailto:hardyjon@msu.edu)

Received: 29 April 2022 Revised: 6 August 2022 Accepted: 30 August 2022

Published online: 20 September 2022

skin rash known as granulomatosis infantiseptica, premature birth, and other neonatal illnesses.<sup>11,17–19</sup> Premature birth has been associated with an increased risk of developing ASD.<sup>20–23</sup> In addition, other severe consequences of listeriosis in the neonate, including meningitis and central nervous system infection, may have severe implications with regard to neurodevelopment. Placental infection by *Lm* causes adverse neurological outcomes in human neonates, including meningism and seizures.<sup>24</sup> In utero, fetal stress due to placental infection by *Lm* could also result in altered neurodevelopment, although long-term consequences of placental listeriosis have not been described.

Sex-specific consequences of placental infection itself in the absence of infection of other tissues have not been defined for any living pathogen. Other prenatal pathogens such as GBS that infect the placenta have been well-studied and have been definitively associated with sex-specific effects on the offspring.<sup>25,26</sup> However, these pathogens also infect other tissues in the reproductive systems in these models, such as the chorioamnion and the amniotic fluid in the case of GBS. In our model, we employ doses in which the placenta is the only reproductive organ infected,<sup>27</sup> and we use imaging to localize the infection. The aims of this study were to understand how *Lm* infection of the placenta affects fetal neurodevelopment, to determine if sex-specific responses occur, and to assess the effects on the behavior of the offspring.

## METHODS

### Animal care and use

All animal procedures were approved by the Institutional Animal Care and Use Committee and the Biosafety of Michigan State University under protocol number 201800030. Michigan State University (MSU) has approved Animal Welfare Assurance (A3955-01) from the NIH Office of Laboratory Animal Welfare (OLAW). Standard BSL-2 containment and handling procedures were used for all animals including the offspring. Timed CD1 pregnant mice (delivered on embryonic day 11) purchased from Charles River Laboratories were used for all studies and housed in temperature controlled, 12:12 h light and dark cycle rooms. Euthanasia was performed by cervical dislocation under isoflurane anesthesia by trained personnel according to NIH and MSU-approved protocols.

### In vivo bioluminescence imaging and tissue processing

The bioluminescent strain of *L. monocytogenes* used in this study (Perkin Elmer Xen32) was generated in a 104035 strain background.<sup>28</sup> Cultures were incubated overnight at 37 °C in brain heart infusion (BHI) broth. The overnight culture was sub-cultured in fresh BHI broth to an optical density (OD<sub>600</sub>) of 0.5. Pregnant CD1 mice were administered a tail vein injection of  $2 \times 10^5$  colony-forming units (CFU) of Xen32, diluted in 200  $\mu$ L phosphate-buffered saline (PBS), or an equivalent volume of PBS vehicle on E14.5. On E18.5, pregnant mice were anesthetized using isoflurane and imaged using the In vivo bioluminescence imaging system (IVIS; Perkin Elmer Inc.), and then humanely sacrificed by cervical dislocation while under isoflurane anesthesia according to the approved animal protocol. Uterine horns were excised immediately and imaged again using the IVIS. Individual fetuses could be imaged separately for high-resolution bioluminescence imaging (BLI). Fetal brains were collected and transferred into sterile Eppendorf tubes, flash-frozen, and stored at –80 °C until analyzed.

### Histology

For histology of the fetal brain, excised fetuses and placentas were imaged with ex-vivo BLI to determine signal levels of the associated placentas. The heads were removed and fixed overnight in 4% paraformaldehyde for sectioning. Following sectioning, the brains were routinely processed and embedded in paraffin and matched coronal sections were stained with hematoxylin and eosin (H&E). Matched coronal sections were also obtained from PBS-injected pregnant mice and from fetuses with and without detectable BLI signals from the placenta from infected pregnant mice. The analysis of alterations in the layering of the brain was performed by counting nuclei in the sex layers of the sections. For each layer, nuclei in six identical 100  $\times$  100  $\mu$ m squares were counted and the same identical squares were used in the matched control sections, for a total of 36 squares per section. For each layer, two-tailed

Student's *t*-test was used to determine statistical significance of the differences between the layers.

### RNA-seq

Total RNA was isolated using the phenol/guanidine-based QIAzol lysis reagent (Qiagen, Valencia, CA), according to the manufacturer's recommendations. The concentration and quality of RNA samples were measured using Qubit (ThermoFisher) and BioAnalyzer (Agilent), respectively. Samples with RNA integrity number values of 9 or above were selected for sequencing. A total of 19 *Lm*-exposed fetal brains from 4 different BLI-positive pregnant mice and 6 fetal brains from PBS control pregnant mice were sequenced. Fetal brains (*Lm*-exposed  $n = 19$ ; control  $n = 6$ ) were collected and total RNA was submitted for next generation sequencing (NGS) library preparation and sequencing to Research Technology Support Facility at MSU. Libraries were prepared using the Illumina TruSeq Standard mRNA Library Preparation Kit with IDT for Illumina Unique Dual Index adapters following manufacturer's recommendations. Completed libraries were quality checked and quantified using a combination of Qubit dsDNA High Sensitivity and Agilent 420 TapeStation HS DNA1000 assays. Libraries were pooled in equimolar proportions for multiplexed sequencing. The pool was quantified using the Kapa Biosystems Illumina Library Quantification qPCR kit. This pool was loaded onto two lanes of an Illumina HiSeq 4000 flow cell (two technical replicates) and sequencing was performed in a 1  $\times$  50 single read format using HiSeq 4000 SBS reagents. Base calling was done by Illumina Real Time Analysis v2.7.7 and output of RTA was demultiplexed and converted to FastQ format with Illumina Bcl2fastq v2.19.1. The raw single-end (SE) reads were processed to trim sequencing adapter and low-quality bases. The clean SE RNA-seq reads were mapped to the mouse reference genome (GCRm38.p6/mm10) using STAR (Spliced Transcripts Alignment to a Reference) v2.3.2.<sup>29</sup> Mapped reads were assigned to genes with FeatureCounts in the subread package.<sup>30</sup>

### Differential gene expression analysis and functional enrichment analysis

Differential gene expression analysis was performed using DESeq2 v1.32.0<sup>31</sup> in R v4.1.1. Genes with minimum 5 raw reads in at least 20 samples were filtered out, resulting a total of 19,180 of genes. Differentially expressed genes with  $p$ -adj < 0.05 were used to perform functional enrichment analysis using the g:Profiler system (<https://biit.cs.ut.ee/gprofiler/gost>).<sup>32</sup> Gene Ontology (GO) enrichment analysis (Biological, Molecular, and Cellular Processes) and KEGG terms with  $p$ -adj < 0.05 were considered significant. To examine the sex dependent effects of placental infection, a female-specific gene, *Xist*, was used to identify the sex of fetal brains from RNA-seq samples. Differential gene expression and functional enrichment analyses were performed using the same parameters as placental infection. Volcano plots were generated using EnhancedVolcano package in R.<sup>33</sup>

### Social interactions and repetitive behaviors

The three-chamber social approach assay has been widely used to test for assaying sociability in mice.<sup>34</sup> This assay measures interaction between animals that are provided choices between unfamiliar animals and inanimate objects (social interaction). We used a custom three-chamber apparatus (63  $\times$  30  $\times$  31 cm) with an empty middle chamber and accessible side chambers on either end that contain cylindrical open barred cages in which mice or objects are placed. An inanimate object is placed in one of the barred cages in one side chamber, and an unfamiliar mouse is placed in the barred cage in the other side chamber. A test subject mouse is placed in the central chamber and allowed to freely interact with the mice or objects in the side chambers. The social interaction test we employed had three phases. First, the test subject (prenatal *Lm*-exposed male = 10 and female = 8; control male = 5 and female = 5) was habituated in the center of the chamber for 10 min and two doorways in the chambers were closed. Second, the test subject was habituated to all three chambers for 10 min. Third, the subject was confined to the middle chamber, a novel object (lab tape) was placed in the barred cage in one side chamber, and a novel mouse (a treatment, sex, and age matched unfamiliar mouse) was placed in the other side chamber.

The social interaction in each test was recorded for 10 min. Sniffing time for each subject was recorded. Self-grooming, which is defined as time spent rubbing the face, scratching with a foot, or licking paws, was examined to measure repetitive and persistent behavior.<sup>34</sup> During the three-chamber social approach assay, self-grooming was measured by

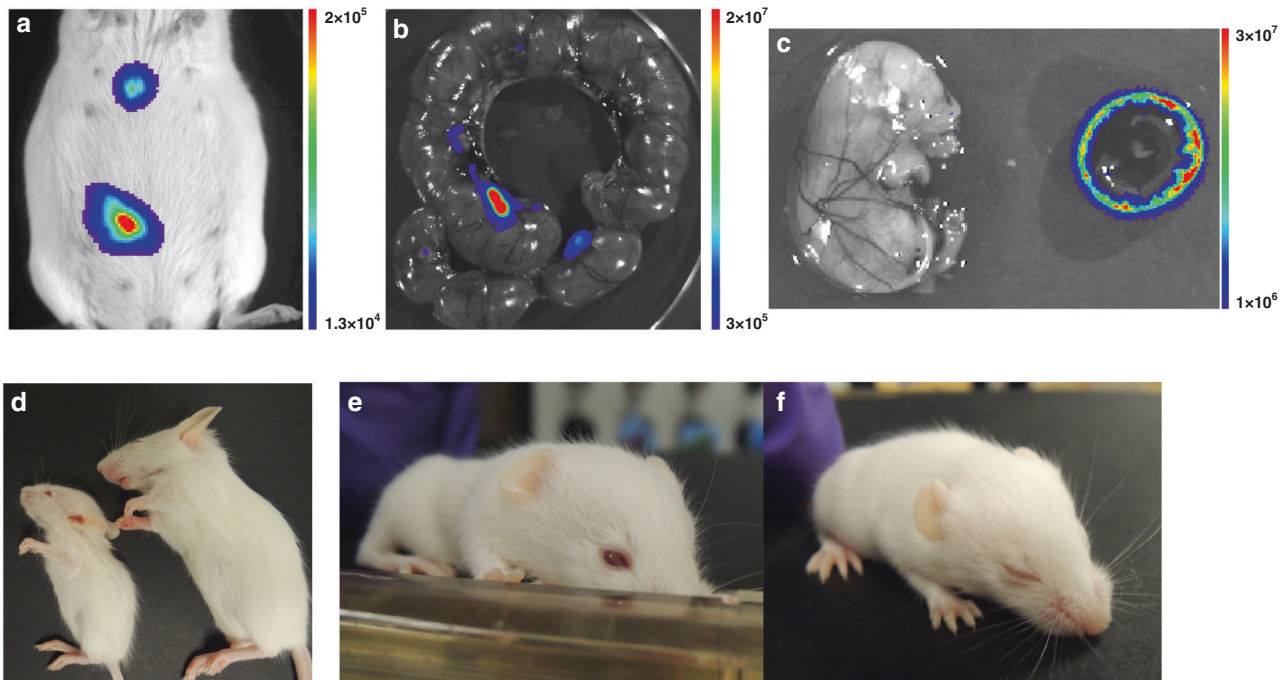


**Fig. 1** Postnatal effects of placental infection. **a–c** In vivo bioluminescence imaging (BLI) of prenatal *L. monocytogenes* (*Lm*) infection. **a** Live pregnant CD1 mouse on embryonic day 18.5 (E.18.5). **b** Excised uterine horns and **c** fetal/placenta pair. **d** Low birth weight due to *Lm* placental infection in a 4-week-old mouse (left) compared to a littermate (right). **e** Control mice exhibit normal eye opening, whereas *Lm*-exposed mice (**f**) are delayed (postnatal day 13).

using a stopwatch. Assessments of social interaction and self-grooming were measured between 8 to 12 weeks of age.<sup>35</sup>

### Open-field exploration

Open-field exploration tests measure anxiety, exploration and locomotion.<sup>36</sup> Mice (prenatal *Lm*-exposed male = 8 and female = 10; control male = 4 and female = 3, 8–12 weeks of age) were acclimated for 30 min before the assay in bright light conditions. Mice were placed in the middle of the testing area (62 × 60 × 31 cm) and underwent a 10-min exploration period. Sessions were video recorded. Time spent in the center (31 × 30 cm) and the total distance traveled (locomotion) were measured using the ANY-maze Video Tracking System software.

## RESULTS

### BLI and postnatal effects of placental infection

All infections were performed by intravenous (IV) injection into pregnant CD1 mice with  $2 \times 10^5$  colony-forming units (CFU) of the bioluminescent *Lm* on E14.5. The dose and timing were selected based on our prior studies.<sup>27</sup> The selected dose results in stillbirth, abortion, and developmental abnormality in some animals, resembling listeriosis in pregnant women. In vivo bioluminescence imaging (BLI) was used to screen the pregnant animals and to localize infection in excised tissues. Mice were separated for analysis based on the BLI signal level obtained by the In Vivo Imaging System (IVIS). An IVIS image of a *Lm*-infected pregnant CD1 mouse is shown in Fig. 1a, with BLI signals indicating different infection sites, including gallbladder and placenta indicated by the intensity of the BLI signals. A description of a cohort can be found in Supplemental Fig. 1. Excised tissues can be imaged to localize the infection (Fig. 1b, c). This process allows tissues to be selected for analysis based on the BLI pattern. The effect of *Lm* infection of the placenta has been described.<sup>27,37</sup> An example of the granulomatous lesions that occur when high BLI signals such as those above  $8 \times 10^5$  photons/s are observed is shown in Supplemental Fig. 2. In addition, BLI demonstrated that *Lm* infection was much greater in the placenta than the fetus (Fig. 1c), as most often at this dose the signal was only

detectable in the placenta and not the fetus. This result was consistent with other studies that showed that fetal infection only occurs at high doses.<sup>11,38</sup> We used vehicle-injected controls to determine the systemic effects of infection, and to show comparisons with normal uninfected animals for histology and gene expression. Fetal and placental pathology in animals with greater than  $5 \times 10^4$  photons/s was consistent with previously published results.<sup>27</sup> At the dose and timing of this study, placental infection was random, with no association with uterine location or sex of the placenta as determined by gene expression. This result is consistent with other models of *Lm* infection, in which low numbers of bacteria seed each organ.<sup>39</sup> Some pups from animals with greater than  $5 \times 10^4$  photons/s showed extreme low birth weight, suggesting postnatal effects of placental infection (Fig. 1d). In animals with less than  $5 \times 10^4$  photons/s, all the mice gave birth 6–12 h before vehicle-injected controls, but the pups were indistinguishable from the controls by weight or any other observable except delayed eye opening (postnatal day 13; Fig. 1e, f).

The range of effects was correlated with overall signal intensities from the live pregnant animal. At the dose we employed, none of the pregnant dams exhibited overt symptoms and they were outwardly indistinguishable from PBS-injected controls. Although some pregnant dams showed BLI signals from the area of the liver and/or gallbladder, all of them survived to give birth if they were allowed to do so. BLI was used to screen the pregnant mice for those to be analyzed for behavioral studies (those below  $5 \times 10^4$  photons/s), because we were not interested in performing these studies on physically abnormal offspring.

### Effect of placental infection on fetal cortical development

To determine whether placental infection promotes morphological changes in the fetal cortex, we performed hematoxylin/eosin (H&E) staining of the cortical sections of fetal brains. We compared fetuses from infected and PBS-injected controls, but also fetuses within single pregnant dams that exhibited high and low signals from the placenta. The latter observation allowed us to distinguish

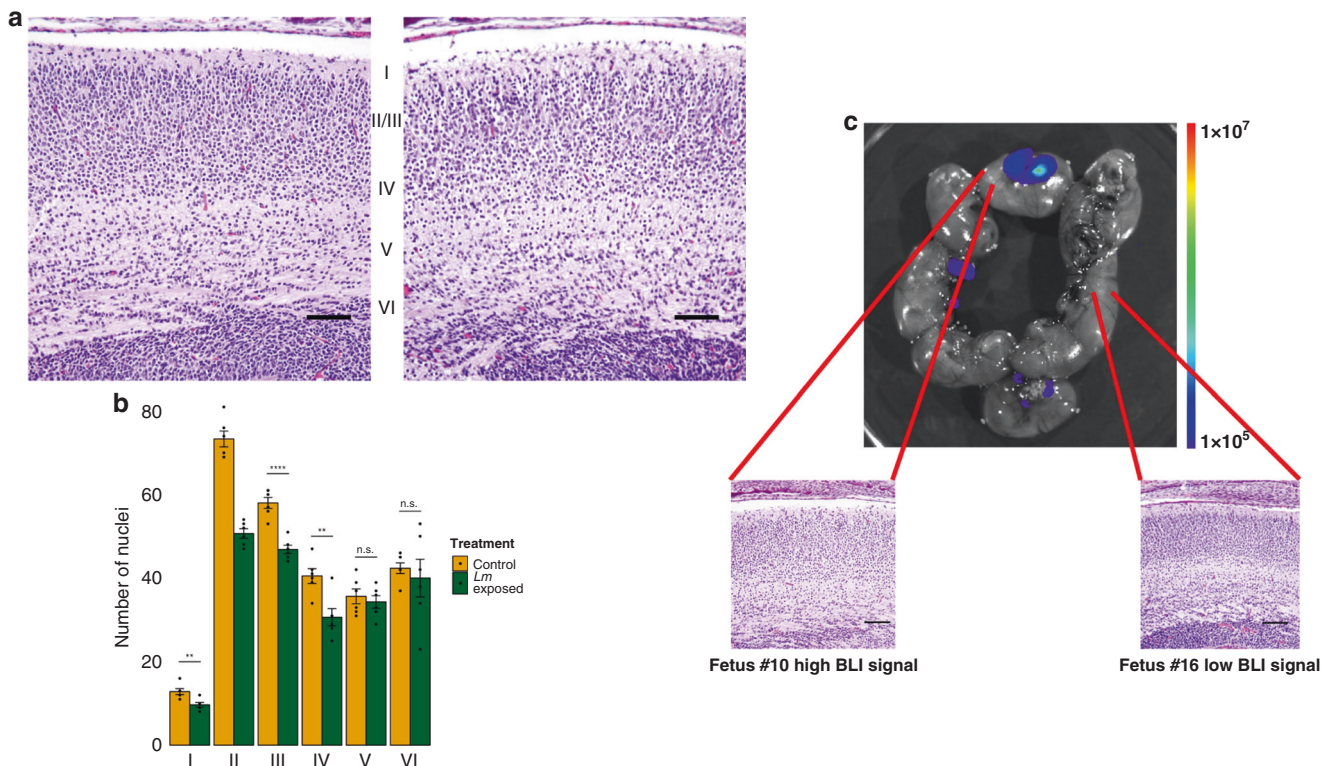


**Fig. 2 Placental infection promotes abnormal cortical lamination.** **a** Coronal sections of fetal brain with normal layering in cortex from PBS-injected pregnant mice (left) and abnormal layering cortex from *Lm*-infected pregnant mice (right). **b** Quantification of nuclei per constant region of interest of cortical layer I–VI. Mean  $\pm$  SEM. Each layer was compared by two-tailed Student's *t*-test: \* $p < 0.05$ , \*\* $p < 0.01$ , \*\*\* $p < 0.001$ , \*\*\*\* $p < 0.0001$ , n.s. = not significant. **c** Abnormal layering in brains from mice with high placental BLI signal versus low placental BLI signal from the same pregnant animal. BLI signal is indicated in photons/s/cm<sup>2</sup>/str. Layers: I: molecular, II: external granular, III: external pyramidal, IV: internal granular, V: internal pyramidal, VI: multiform. Scale bars: **a** = 100  $\mu$ m; **c** = 200  $\mu$ m.

effects due to systemic MIA from localized effects of the placenta. In the sections, layering was abnormal in the fetal brains from mice that originated from infected dams compared to controls (Fig. 2a). We analyzed alterations in layering by counting nuclei in fixed 100  $\times$  100  $\mu$ m regions of interest and comparing the numbers of nuclei in each layer to corresponding layers in controls (Fig. 2b). The scheme for this analysis is shown in Supplemental Fig. 3. *Lm*-exposed fetal brains showed a statistically significant decrease in number of nuclei layers I–IV, but not in layers V or VI. Fetal brains from mice where the placentas exhibiting BLI signals above background showed layering alterations compared to fetuses from the same dam where the placenta had background BLI signals from the same dam (Fig. 2b).

### Infection of the placenta alters gene expression in the fetal mouse brain

We next investigated the effect of placental infection on transcriptomic alterations in fetal brain. For these investigations, we used fetal brains from mice in which no BLI signal over background was detectable in the brain. A total of 25 whole fetal brains (6 control and 19 *Lm*-exposed samples) were harvested on E18.5 from four different pregnant mice to generate RNA-seq datasets and performed differential expression analysis using a DESeq2 package in R. The analysis revealed that IV injection of bioluminescent *Lm* into pregnant CD1 mice at E14.5 altered gene expression in the fetal mouse brain. Overall, *Lm*-exposed fetal brains had a total of 268 upregulated and 139 downregulated differentially expressed genes (DEGs) with a false discover rate (FDR)  $< 0.05$  threshold, and 1697 upregulated and 1247 downregulated with a  $p < 0.05$  threshold (Fig. 3a). Among DEGs, most significant genes include upregulated *Lyrm7*, *Flt1*, *Vegfa*, and

*Kdm3a*, and downregulated *Zfp125*, *Mfsd5*, *slc38a5*, *Mblac1*, and *Chd15* (Fig. 3b). The Gene Ontology (GO) enrichment and KEGG analysis of upregulated DEGs revealed pathways, such as macromolecule biosynthetic and nitrogen compound metabolic processes, and hypoxia inducible factor-1 (HIF-1) signaling pathway (Fig. 3c). Furthermore, pathways such as establishment of localization in cell and protein processing in endoplasmic reticulum were identified among significantly downregulated DEGs (Fig. 3c). Many of these genes are associated with brain development or neurological function.<sup>40–43</sup> Together, differential expression analysis demonstrated that placental infection by *Lm* causes disruption of neurodevelopment during pregnancy.

### Male and female fetal brains exhibit distinct gene expression profiles in response to placental infection

We used *Xist*, a female-specific gene, to identify sex of each fetal brain RNA-seq sample (males: 9 *Lm*-exposed and 3 controls; females: 10 *Lm*-exposed and 3 controls). We used DESeq2 in R to identify DEGs and investigated overlapping genes between both *Lm*-exposed sexes. A total of 44 and 42 downregulated DEGs were identified for males and females, respectively, with one gene overlapping between the sexes (Fig. 4a). Interestingly, females had 171 upregulated DEGs while males had 50 upregulated DEGs with 7 DEGs overlapping between the sexes (Fig. 4b). GO enrichment and KEGG analysis of upregulated DEGs of *Lm*-exposed male fetal brains identified pathways, such as VEGF receptor 2 binding, HIF-1 signaling, and microtubule organizing center (Fig. 4c). In addition, ribosome, mitochondrial translation elongation and termination, and oligosaccharyltransferase complex pathways were identified in downregulated DEGs of *Lm*-exposed male fetal brains (Fig. 4d). Analysis of the GO enrichment and KEGG analyses of upregulated

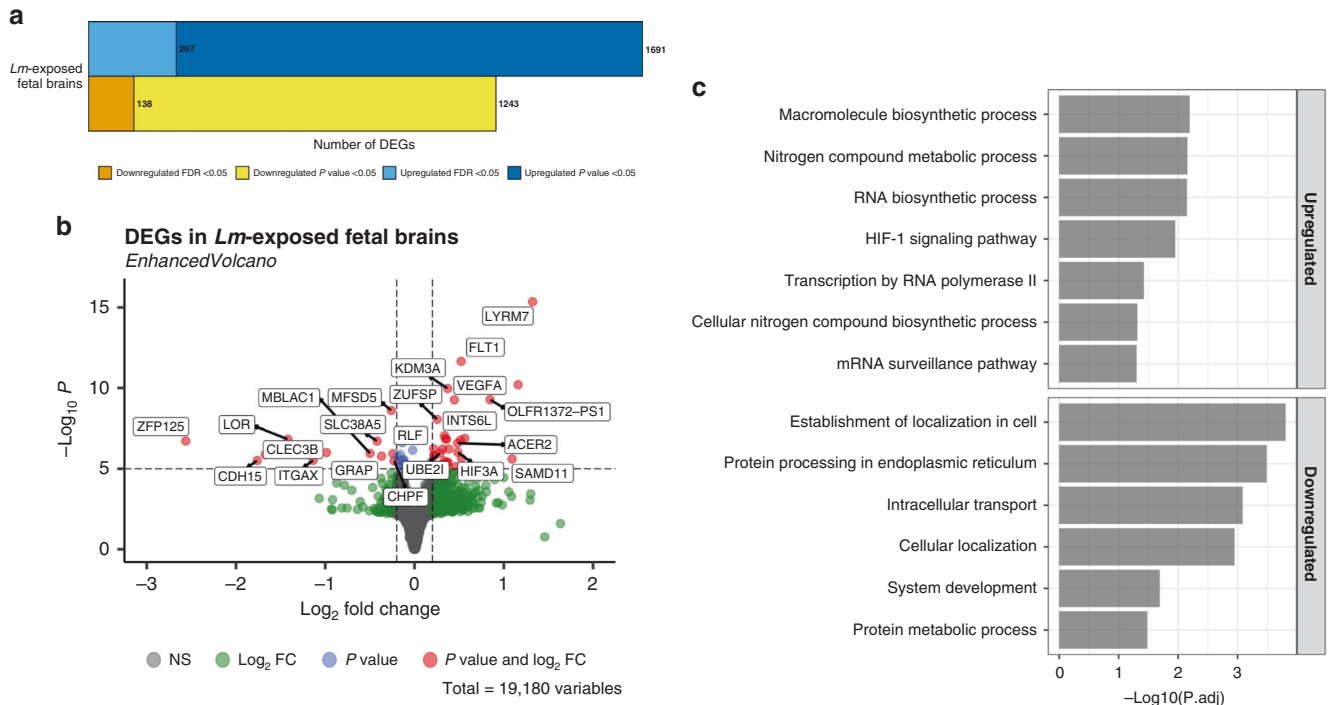


**Fig. 3** Gene expression changes in the fetal brain due to placental infection with *Lm*. **a** Total number of differentially expressed genes (DEGs) of fetal brains in response to placental infection. **b** Volcano plot of DEGs in *Lm*-exposed fetal brains of *Lm*-exposed mice at E18.5. Red dots indicate statistical significance ( $p$ -value <  $10^6$ ) and  $\log_2$ (fold-change) greater or less than 0.2. Total variables indicate the total number of genes that were used to generate a volcano plot. **c** Gene set enrichment analysis of GO and KEGG terms of DEGs ( $p$ -adj < 0.05) in fetal brains of *Lm*-exposed mice at E18.5. Biological pathways of downregulated and upregulated fetal brains of *Lm*-exposed mice were identified using g:ProfileR.

DEGs in *Lm*-exposed female fetal brains demonstrated organelle related and nuclear speck pathways, whereas catenin complex and postsynaptic actin cytoskeleton pathways were identified in downregulated DEGs (Fig. 4c, d). These findings demonstrated that placental infection had different effects on male versus female brains during neurodevelopment.

### Placental infection induces sex-specific behavioral alterations in adult offspring

We sought to determine if altered behaviors were induced in the progeny of dams infected with *Lm*. Bacterial chorioamnionitis, which is not placental, leads to autism-like alterations in the behavior of progeny in animals,<sup>25</sup> so we selected behavioral tests that are used as correlates for human ASD. For this purpose, we screened the pregnant dams with BLI to identify those with signals less than  $4 \times 10^4$  photons/s. These mice give birth to normal-sized pups, which cannot be grossly distinguished from controls from PBS-injected dams. When the pups were 8 to 12 weeks of age, we performed behavioral assays to determine if the adult mouse offspring exhibited abnormal behavioral due to placental infection by *Lm*. First, we analyzed social interaction by using the three-chamber social approach assay to assess social impairment. *Lm*-exposed male adult offspring presented with a significant reduction in social interaction time with an unfamiliar mouse, whereas *Lm*-exposed female adult offspring did not (Fig. 5a; two-way ANOVA,  $p = 0.016$  by Tukey's HSD test). We cannot rule out the olfaction was affected by placental infection by *Lm*, which may alter these responses. If so, the effect would appear to be sex-specific.

To assess repetitive behavior, the duration of self-grooming was examined during the three-chamber social approach assay. Self-grooming in rodents has been used as a surrogate for repetitive behavior in humans with ASD.<sup>44–46</sup> *Lm*-exposed male adult offspring spent significantly more time self-grooming compared to the PBS treated male mice (Fig. 5b; two-way ANOVA,  $p = 0.044$  by

Tukey's HSD test). However, self-grooming behavior of female adult offspring was not affected by prenatal *Lm* exposure.

Next, we examined the level of anxiety and locomotion using an open-field exploration test. Higher level of thigmotaxis, a subject remaining close to walls, is usually indicative of heightened anxiety.<sup>47</sup> Compared with PBS treated controls, *Lm*-exposed female adult offspring spent less time in the center of the field (two-way ANOVA,  $p = 0.011$  by post hoc test). However, *Lm*-exposed male adult offspring did not show difference in total time spent in the center compared to the PBS treated male group (Fig. 5c). In addition, both *Lm*-exposed male and female groups showed no difference in total travel distance, which indicates locomotion activity was not affected (Fig. 5e). Together, placental infection causes abnormal behaviors in offspring that are relevant to human neuropsychiatric disorder symptoms, including elevated anxiety, increased repetitive behavior, and impaired social interaction.

### DISCUSSION

Although listeriosis may cause serious and even fatal consequences for pregnant women and their offspring, its effect on neurodevelopment of the adult offspring has not been characterized. Here, we used bioluminescent *Lm* and the IVIS imaging system to determine if placental infection affects fetal neurodevelopment and the behavior of offspring in mice. We have long observed alterations in the structure of the fetal brain due to placental infection by *Lm*. Upon quantifying these alterations, it became apparent that the four outer layers of the brain exhibited more abnormality than the two innermost layers (Fig. 2). This interesting finding may indicate an alteration of neuronal motility, as this process occurs from the inside out. Immune modulation by *Lm* is likely to cause many of the effects we observe in fetal brain structure, as the MIA models have clearly demonstrated the role of immune mediators. It is very likely that immune-mediated placental dysfunction is responsible for the

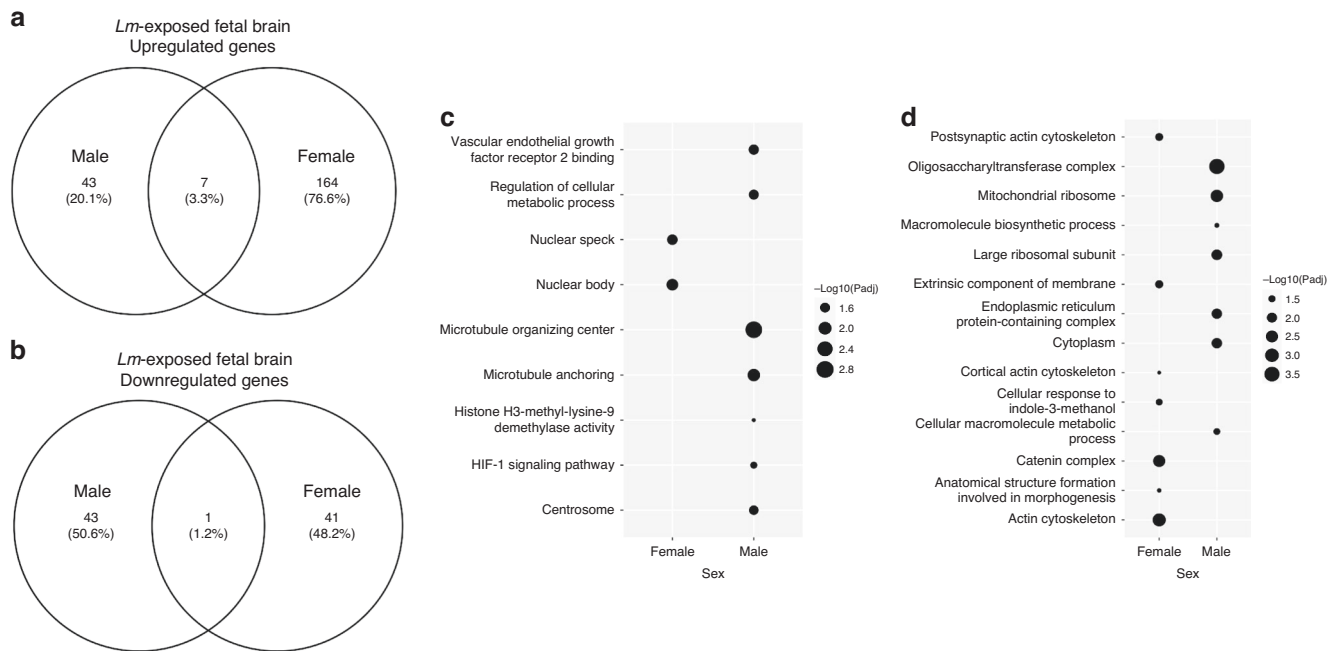


**Fig. 4 Sexually dichotomous gene expression profiles induced by placental infection.** **a, b** Venn Diagrams representing the number of overlapping downregulated and upregulated genes in **a** and **b**, respectively. **c, d** Enrichment analysis of DEGs ( $p$ -adj < 0.05) of fetal brains from female and male *Lm*-exposed mice. Gene set enrichment analysis of upregulated and downregulated GO and KEGG terms are shown in **c** and **d**, respectively.

effects we observe, and placental analysis will reveal details of this process.

The identification of biological pathways in exposed whole brain transcriptome data suggests that placental infection with *Lm* dysregulates transcriptional levels of several different processes during neurodevelopment. HIF-1 signaling pathway was upregulated, suggesting placental infection induces hypoxic conditions in the fetal brain during neurodevelopment. Dysregulation of these genes has been identified in neuropsychiatric disorders<sup>42,48</sup> Protein processing in the endoplasmic reticulum (ER) pathway was downregulated due to placental infection by *Lm*. Dysregulation of protein synthesis has previously been suggested as one of the cellular responses to a hypoxic condition<sup>49</sup> and implicated in various neuropsychiatric disorders.<sup>50</sup> Furthermore, a recent study found that poly(I:C) induced MIA triggers ER stress as a cellular response to inflammation and results in reduced protein synthesis.<sup>51</sup> Sexual dimorphism in neuropsychiatric disorders is well recognized. However, the basis of this dichotomy is unknown. Recent MIA studies demonstrate that inflammation during pregnancy caused sex-biased placental and fetal pro-inflammatory responses.<sup>6</sup> Consistent with previous MIA study, upregulation of HIF-1 signaling pathway was only enriched in *Lm*-exposed males, suggesting males may be more susceptible to hypoxia during pregnancy. Future work should examine at the protein level by performing proteomic analysis to better understand how male and female brain development is impacted by *Lm* infection during pregnancy.

Similar to MIA-associated studies, *Lm*-exposed male offspring, but not female offspring, showed a significant reduction in social interaction and more frequent repetitive behaviors (Fig. 5a, b). These behavioral changes, and male-biased sex ratio, are observed in human ASD patients. Interestingly, we only observed significantly increased anxiety levels in *Lm*-exposed female offspring (Fig. 5d), whereas MIA-associated male offspring exhibited heightened anxiety levels during open-field exploration. It is important to note that numerous MIA studies have investigated behavioral changes only using male offspring<sup>52–54</sup> because the prevalence of developing ASD is higher in males than in females. This difference remains to be further investigated; however, women are more likely to be

diagnosed with some anxiety disorders.<sup>55</sup> Another behavioral discrepancy was observed in locomotor activity. In our studies, placental infection did not alter locomotor activity in either sex. Interestingly, Allard et al. demonstrated that prenatal infection with live Group B *Streptococcus*, a major health concern during pregnancy implicated in preterm birth and stillbirth, led to hyperlocomotor and elevated anxiety behaviors in male rat offspring, but not in female rat offspring.<sup>25</sup> Our contrasting results highlight the need to examine diverse prenatal pathogens, as it is becoming clear that different infections result in distinct neurological abnormalities. However, it is important to note that different species were used to investigate locomotion activity in our experiments.

One of the limitations of our studies is that individual placental BLI signals cannot be correlated with the behavior of individual offspring. Although the BLI signal of the pregnant dam can be measured using an IVIS, severity of each placental infection cannot be quantified except by sacrificing the animal. In our model, individual placentas are differentially infected by *Lm* (Fig. 1b), and our previous findings show that fetal pathologies, such as bradycardia and fetal resorption, are correlated with BLI signals from pregnant dams. Another limitation of this study is the dose and timing of *Lm* infection we selected, which could be varied to examine the effects of severity and timing. We have not studied the consequences of direct infection of the fetal brain, which occurs in mice with higher BLI signals, nor the effect of infection of maternal organs such as the liver or spleen, which would induce MIA.

In summary, we have established that placental infection by *Listeria* affects the trajectory of fetal neurodevelopment during pregnancy. We observed sex-specific dysregulation of the fetal brain transcriptome due to *Lm* infection during pregnancy. We also demonstrated that prenatal infection causes sex-specific behavioral abnormalities in offspring that resemble human ASD and anxiety-related disorders, which are known to have sexually dimorphic effects. Altogether, we have identified neurodevelopmental effects of placental infection by *Lm* and expanded models of prenatal infection-associated sexual dimorphism of behavior, thus improving our understanding of the development of neuropsychiatric disorders.

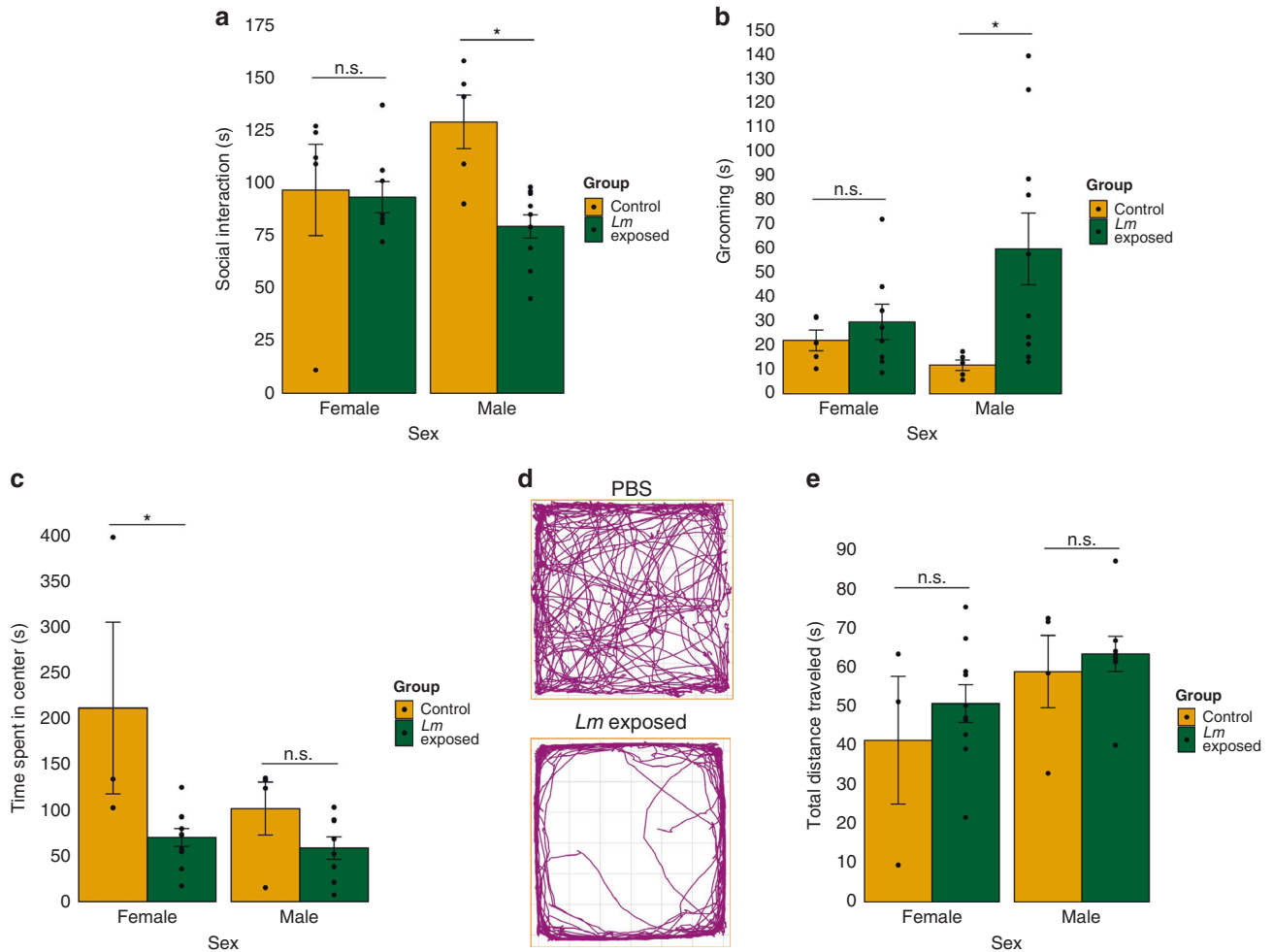


**Fig. 5 Sex-specific abnormal behaviors in the offspring of *Lm*-infected pregnant mice.** **a** *Lm*-exposed adult male mouse offspring display deficits in social interaction (sniffing of unfamiliar mice versus inanimate objects) whereas *Lm*-exposed adult female mouse offspring show no altered behavior. **b** *Lm*-exposed adult male mouse offspring exhibit high levels of grooming (resembles repetitive behavior). Number (*n*) of offspring: control male (*n* = 5), *Lm*-exposed male (*n* = 10), control female (*n* = 5), and *Lm*-exposed female (*n* = 8) (**a**, **b**). **c** Heightened level of anxiety observed only in *Lm*-exposed adult female mouse offspring. **d** Differences in tracked movement during the open-field exploration assay in *Lm*-exposed adult mouse offspring versus PBS controls. **e** No significant change in total distance traveled during open-field exploration. Control male (*n* = 3), *Lm*-exposed male (*n* = 8), control female (*n* = 3), and *Lm*-exposed female (*n* = 10) used in open-field exploration. Data are shown as the mean  $\pm$  SEM. The behavioral assay data were analyzed by two-way analysis of variance (ANOVA) followed by Tukey's HSD test. \**P* < 0.05., ns = not significant.

## DATA AVAILABILITY

The datasets, including RNA-seq fastq and raw counts of sequencing reads, can be accessed through the NCBI Gene Expression Omnibus, accession number GSE213619.

## REFERENCES

- Atladóttir, H. Ó. et al. Maternal infection requiring hospitalization during pregnancy and autism spectrum disorders. *J. Autism Dev. Disord.* **40**, 1423–1430 (2010).
- Brown, A. S. et al. Serologic evidence of prenatal influenza in the etiology of schizophrenia. *Arch. Gen. Psychiatry* **61**, 774–780 (2004).
- Sørensen, H. J., Mortensen, E. L., Reinisch, J. M. & Mednick, S. A. Association between prenatal exposure to bacterial infection and risk of Schizophrenia. *Schizophr. Bull.* **35**, 631–637 (2009).
- Canales, C. P. et al. Sequential perturbations to mouse corticogenesis following in utero maternal immune activation. *Elife* **10**, 1–27 (2021).
- Choi, G. B. et al. The maternal interleukin-17a pathway in mice promotes autism-like phenotypes in offspring. *Science (80-)*. **351**, 933–939 (2016).
- Braun, A. E. et al. "Females are not just 'Protected' Males": Sex-specific vulnerabilities in placenta and brain after prenatal immune disruption. *eNeuro* **6**, ENEURO.0358-19 (2019).
- Makinson, R. et al. Intrauterine inflammation induces sex-specific effects on neuroinflammation, white matter, and behavior. *Brain. Behav. Immun.* **66**, 277–288 (2017).
- Bergeron, J. D. L. et al. White matter injury and autistic-like behavior predominantly affecting male rat offspring exposed to group B streptococcal maternal inflammation. *Dev. Neurosci.* **35**, 504–515 (2013).
- Brown, A. S., Schaefer, C. A., Quesenberry, C. P., Shen, L. & Susser, E. S. No evidence of relation between maternal exposure to herpes simplex virus type 2 and risk of schizophrenia? *Am. J. Psychiatry* **163**, 2178–2180 (2006).
- Khandaker, G. M., Zimbron, J., Lewis, G. & Jones, P. B. Prenatal maternal infection, neurodevelopment and adult schizophrenia: a systematic review of population-based studies. *Psychol. Med.* **43**, 239–257 (2013).
- Bakardjiev, A. I., Theriot, J. A. & Portnoy, D. A. *Listeria monocytogenes* traffics from maternal organs to the placenta and back. *PLoS Pathog.* **2**, 0623–0631 (2006).
- Hamrick, T. S. et al. Influence of pregnancy on the pathogenesis of listeriosis in mice inoculated intragastrically. *Infect. Immun.* **71**, 5202–5209 (2003).
- CDC. People at Risk—Pregnant Women and Newborns | *Listeria* | CDC. Available at: <https://www.cdc.gov/listeria/risk-groups/pregnant-women.html> (accessed: 5th March 2022).
- Lecuit, M. Understanding how *Listeria monocytogenes* targets and crosses host barriers. *Clin. Microbiol. Infect.* **11**, 430–436 (2005).
- Robbins, J. R., Skrzyzyczna, K. M., Zeldovich, V. B., Kapidzic, M. & Bakardjiev, A. I. Placental syncytiotrophoblast constitutes a major barrier to vertical transmission of *Listeria monocytogenes*. *PLoS Pathog.* **6**, e1000732 (2010).

16. Johnson, L. J. et al. Human placental trophoblasts infected by listeria monocytogenes undergo a pro-inflammatory switch associated with poor pregnancy outcomes. *Front. Immunol.* **12**, 1–21 (2021).
17. Goldenberg, R. L., Culhane, J. F. & Johnson, D. C. Maternal infection and adverse fetal and neonatal outcomes. *Clin. Perinatol.* **32**, 523–559 (2005).
18. Lamont, R. F. et al. Listeriosis in human pregnancy. *J. Perinat. Med.* **39**, 227–236 (2011).
19. Charlier, C., Disson, O. & Lecuit, M. Maternal-neonatal listeriosis. *Virulence* **11**, 391–397 (2020).
20. Crump, C., Sundquist, J. & Sundquist, K. Preterm or early term birth and risk of autism. *Pediatrics* **148**, e2020032300 (2021).
21. Leavey, A., Zwaigenbaum, L., Heavner, K. & Burstyn, I. Gestational age at birth and risk of autism spectrum disorders in Alberta, Canada. *J. Pediatr.* **162**, 361–368 (2013).
22. Chen, L. W. et al. Behavioral characteristics of autism spectrum disorder in very preterm birth children. *Mol. Autism* **10**, 1–9 (2019).
23. Agrawal, S., Rao, S. C., Bulsara, M. K. & Patole, S. K. Prevalence of autism spectrum disorder in preterm infants: a meta-Analysis. *Pediatrics* **142**, e20180134 (2018).
24. Mylonakis, E., Paliou, M., Hohmann, E. L., Calderwood, S. B. & Wing, E. J. Listeriosis during pregnancy: a case series and review of 222 cases. *Medicine (Baltim.)* **81**, 260–269 (2002).
25. Allard, M. J. et al. A sexually dichotomous, autistic-like phenotype is induced by Group B Streptococcus maternofetal immune activation. *Autism Res.* **10**, 233–245 (2017).
26. Allard, M. J., Giraud, A., Segura, M. & Sebire, G. Sex-specific maternofetal innate immune responses triggered by group B Streptococci. *Sci. Rep.* **9**, 1–13 (2019).
27. Hardy, J. et al. Infection of pregnant mice with listeria monocytogenes induces fetal bradycardia. *Pediatr. Res.* **71**, 539–545 (2012).
28. Hardy, J. et al. Extracellular replication of listeria monocytogenes in the murine gall bladder. *Science. (80-.)* **303**, 851–853 (2004).
29. Dobin, A. et al. STAR: Ultrafast universal RNA-seq aligner. *Bioinformatics* **29**, 15–21 (2013).
30. Liao, Y., Smyth, G. K. & Shi, W. FeatureCounts: an efficient general purpose program for assigning sequence reads to genomic features. *Bioinformatics* **30**, 923–930 (2014).
31. Love, M. I., Huber, W. & Anders, S. Moderated estimation of fold change and dispersion for RNA-seq data with DESeq2. *Genome Biol.* **15**, 1–21 (2014).
32. Raudvere, U. et al. G:Profiler: a web server for functional enrichment analysis and conversions of gene lists (2019 update). *Nucleic Acids Res.* **47**, W191–W198 (2019).
33. Blighe, K., Rana, S. & Lewis, M. EnhancedVolcano: Publication-ready volcano plots with enhanced colouring and labeling. Available at: <https://github.com/kevinblighe/EnhancedVolcano> (accessed: 7th March 2022).
34. Yang, M., Silverman, J. L. & Crawley, J. N. Automated three-chambered social approach task for mice. *Curr. Protoc. Neurosci.* 1–16, <https://doi.org/10.1002/0471142301.ns0826s56> (2011).
35. Kaidanovich-Beilin, O., Lipina, T., Vukobradovic, I., Roder, J. & Woodgett, J. R. Assessment of social interaction behaviors. *J. Vis. Exp.* **0**, 1–6 (2010).
36. Seibenhener, M. L. & Wooten, M. C. Use of the open field maze to measure locomotor and anxiety-like behavior in mice. *J. Vis. Exp.* 1–6, <https://doi.org/10.3791/52434> (2015).
37. Bakardjiev, A. I., Stacy, B. A., Fisher, S. J. & Portnoy, D. A. Listeriosis in the pregnant guinea pig: a model of vertical transmission. *Infect. Immun.* **72**, 489–497 (2004).
38. Le Monnier, A., Join-Lambert, O. F., Jaubert, F., Berche, P. & Kayal, S. Invasion of the placenta during murine listeriosis. *Infect. Immun.* **74**, 663–672 (2006).
39. Zhang, T. et al. Deciphering the landscape of host barriers to Listeria monocytogenes infection. *Proc. Natl Acad. Sci. USA* **114**, 6334–6339 (2017).
40. Bhalla, K. et al. Alterations in CDH15 and KIRREL3 in Patients with Mild to Severe Intellectual Disability. *Am. J. Hum. Genet.* **83**, 703–713 (2008).
41. Kim, J. H., Lee, J. H., Lee, I. S., Lee, S. B. & Cho, K. S. Histone lysine methylation and neurodevelopmental disorders. *Int. J. Mol. Sci.* **18**, 1–20 (2017).
42. Lange, C., Storkebaum, E., De Almodovar, C. R., Dewerchin, M. & Carmeliet, P. Vascular endothelial growth factor: A neurovascular target in neurological diseases. *Nat. Rev. Neurol.* **12**, 439–454 (2016).
43. Fernandes, A. et al. Hypoxia-inducible factor (HIF) in ischemic stroke and neurodegenerative disease. *Front. Cell Dev. Biol.* 9:703084 (2021).
44. Kaluff, A. V. et al. Neurobiology of rodent self-grooming and its value for translational neuroscience. *Nat. Rev. Neurosci.* **17**, 45–59 (2016).
45. Arakawa, H. Implication of the social function of excessive self-grooming behavior in BTBR T+Itpr3tf/J mice as an idiopathic model of autism. *Physiol. Behav.* **237**, 113432 (2021).
46. Gandhi, T. & Lee, C. C. Neural mechanisms underlying repetitive behaviors in rodent models of autism spectrum disorders. *Front. Cell. Neurosci.* **14**, 1–44 (2021).
47. Simon, P., Dupuis, R. & Costentin, J. Thigmotaxis as an index of anxiety in mice. Influence of dopaminergic transmissions. *Behav. Brain Res.* **61**, 59–64 (1994).
48. Carmeliet, P. & Storkebaum, E. Vascular and neuronal effects of VEGF in the nervous system: Implications for neurological disorders. *Semin. Cell Dev. Biol.* **13**, 39–53 (2002).
49. Koumenis, C. et al. Regulation of protein synthesis by hypoxia via activation of the endoplasmic reticulum kinase PERK and phosphorylation of the translation initiation factor eIF2 $\alpha$ . *Mol. Cell. Biol.* **22**, 7405–7416 (2002).
50. Laguesse, S. & Ron, D. Protein translation and psychiatric disorders. *Neuroscientist* **26**, 21–42 (2020).
51. Kalish, B. T. et al. Maternal immune activation in mice disrupts proteostasis in the fetal brain. *Nat. Neurosci.* **24**, 204–213 (2021).
52. Zuckerman, L. & Weiner, I. Maternal immune activation leads to behavioral and pharmacological changes in the adult offspring. *J. Psychiatr. Res.* **39**, 311–323 (2005).
53. Meyer, U. et al. Adult behavioral and pharmacological dysfunctions following disruption of the fetal brain balance between pro-inflammatory and IL-10-mediated anti-inflammatory signaling. *Mol. Psychiatry* **13**, 208–221 (2008).
54. Wolff, A. R., Cheyne, K. R. & Bilkey, D. K. Behavioural deficits associated with maternal immune activation in the rat model of schizophrenia. *Behav. Brain Res.* **225**, 382–387 (2011).
55. McLean, C. P., Asnaani, A., Litz, B. T. & Hofmann, S. G. Gender differences in anxiety disorders: prevalence, course of illness, comorbidity and burden of illness. *J. Psychiatr. Res.* **45**, 1027–1035 (2011).

## ACKNOWLEDGEMENTS

The authors would like to acknowledge Dr. Kevin Childs, the director of Genomics Core at MSU for consulting regarding the RNA-seq experiment. Additionally, we also acknowledge Dr. Alexa Veenema for the help with behavioral assays.

## AUTHOR CONTRIBUTIONS

K.H.L. designed the experiment, performed experiments, collected data, wrote the draft and edited the manuscript. M.K and T.W. design and executed experiments and helped write the manuscript. P.P. designed and executed experiments and contributed to writing the manuscript. J.H. conceptualized the project, supervised the team with feedback and evaluation of the project, edited the manuscript. All authors read and approved the final manuscript.

## FUNDING

This work has partly supported by the March of Dimes Prematurity Research Center at Stanford University, and partly by Michigan State University Startup Funds for Jonathan Hardy.

## COMPETING INTERESTS

The authors declare no competing interests.

## ETHICS APPROVAL AND CONSENT TO PARTICIPATE

No human patients were involved in this study. All animal procedures were approved by Institutional Animal Care and Use Committee and the Biosafety Committee of Michigan State University under animal protocol number 201800030.

## ADDITIONAL INFORMATION

**Supplementary information** The online version contains supplementary material available at <https://doi.org/10.1038/s41390-022-02307-1>.

**Correspondence** and requests for materials should be addressed to Jonathan Hardy.

**Reprints and permission information** is available at <http://www.nature.com/reprints>

**Publisher's note** Springer Nature remains neutral with regard to jurisdictional claims in published maps and institutional affiliations.

Springer Nature or its licensor holds exclusive rights to this article under a publishing agreement with the author(s) or other rightsholder(s); author self-archiving of the accepted manuscript version of this article is solely governed by the terms of such publishing agreement and applicable law.